Hyperforin modulates MAPK/CCL11 signaling to reduce the inflammatory response of nasal mucosal epithelial cells caused by allergic rhinitis by targeting BCL6

CHEN XU and WEN SU

Department of Pediatrics, Wuhan Hospital of Integrated Traditional Chinese and Western Medicine (Wuhan No. 1 Hospital), Wuhan, Hubei 430022, P.R. China

Received February 23, 2023; Accepted August 17, 2023

DOI: 10.3892/etm.2023.12278

Abstract. Hyperforin is a type of bicyclic tetraketone with four isoprenoid chains extracted from *Hypericum perforatum* L. that has multiple biological activities such as anti-diabetes, antitumor and anti-inflammation. However, the role and potential mechanism of hyperforin in allergic rhinitis (AR) remains to be clarified. In the present study, cell viability was analyzed using Cell Counting Kit-8 assay, while inflammation was detected using ELISA and reverse transcription-quantitative PCR. Epithelial cell barrier damage was measured using western blotting and immunofluorescence staining. The expression levels of B-cell lymphoma 6 (BCL6) and the p38 MAPK/C-C motif chemokine 11 (CCL11) pathway were detected using western blotting. In addition, the association between hyperforin and BCL6 was analyzed by SWISS TargetPrediction, DisGeNET, Gene Ontology and Pathway databases. Molecular docking was performed using AutoDockTools 1.5.6 and Discovery Studio 4.5 software. The data demonstrated that there were 16 interlinking target genes of hyperforin with AR, in which BCL6 was the most relevant one with hyperforin in AR. The binding between hyperforin and BCL6 was verified, and molecular docking was modeled. The results revealed that hyperforin inhibited IL-13-induced nasal epithelial inflammatory cytokine release and repressed the damage to the cellular barrier from IL-13 stimulation. In addition, hyperforin activated BCL6 expression and significantly suppressed the expression of p38 MAPK/CCL11. Silencing of BCL6 reversed the effects of hyperforin on IL-13-induced inflammation and barrier damage. In summary, the present results revealed that hyperforin suppressed IL-13-induced nasal epithelial cell inflammation and barrier damage by targeting BCL6/p38 MAPK/CCL11, which may provide promising therapeutic targets for AR.

Correspondence to: Dr Wen Su, Department of Pediatrics, Wuhan Hospital of Integrated Traditional Chinese and Western Medicine (Wuhan No. 1 Hospital), 215 Zhongshan Avenue, Qiaokou, Wuhan, Hubei 430022, P.R. China
E-mail: suwen930215@163.com

Key words: hyperforin, allergic rhinitis, B-cell lymphoma 6, p38 MAPK, C-C motif chemokine 11

Introduction

Allergic rhinitis (AR) is one of the most common nasal diseases in the world, and is usually endured throughout life (1). It is estimated that the prevalence of AR accounts for 10-30% of the global population (2). AR is defined as an immunoglobulin E (IgE)-mediated inflammatory disease of the nasal mucosa caused by allergen exposure, and is characterized by sneezing, nasal congestion, itching and rhinorrhea (3).

In classical AR pathophysiology, elevated allergen specific IgE levels and T-helper (Th) 1/Th2 imbalance are considered to be major deviant immune factors (4). Epithelial cells play a key protective role, since they are the first physiological barrier against allergen infiltration (5). Th2 cytokines also induce the breakdown of the epithelial barrier in allergic diseases, and epithelial cells release cytokines to promote Th2 immune response (6). Therefore, preservation of the epithelial barrier function can reduce the type 2 immune response caused by the influx of harmful environmental molecules, including allergens, which is considered as a promising therapeutic strategy for AR therapy (7).

Hyperforin, a bicyclic tetraketone with four isoprenoid chains, is a major active constituent of *Hypericum perforatum* L. (8). It is also known as St. John's wort, and is widely used for the treatment of depressive disorders (9). In recent years, it has been revealed that hyperforin has various pharmacological activities, such as anti-diabetic, antitumor and anti-dementia activities (10-12). In addition, hyperforin has been revealed to have anti-inflammatory properties and is resistant to barrier damage. For instance, hyperforin can improve imiquimod-induced psoriasis-like skin inflammation in mice by regulating γδ T cells that produce IL-17A (13). Moreover, hyperforin promotes the expression of tight junction proteins in endothelial cells after blood-brain barrier injury (14). However, whether hyperforin is involved in nasal epithelial cell damage caused by AR is unknown. Thus, the present study aimed to explore the functional roles of hyperforin on IL-13-stimulated nasal epithelial cells and discuss the

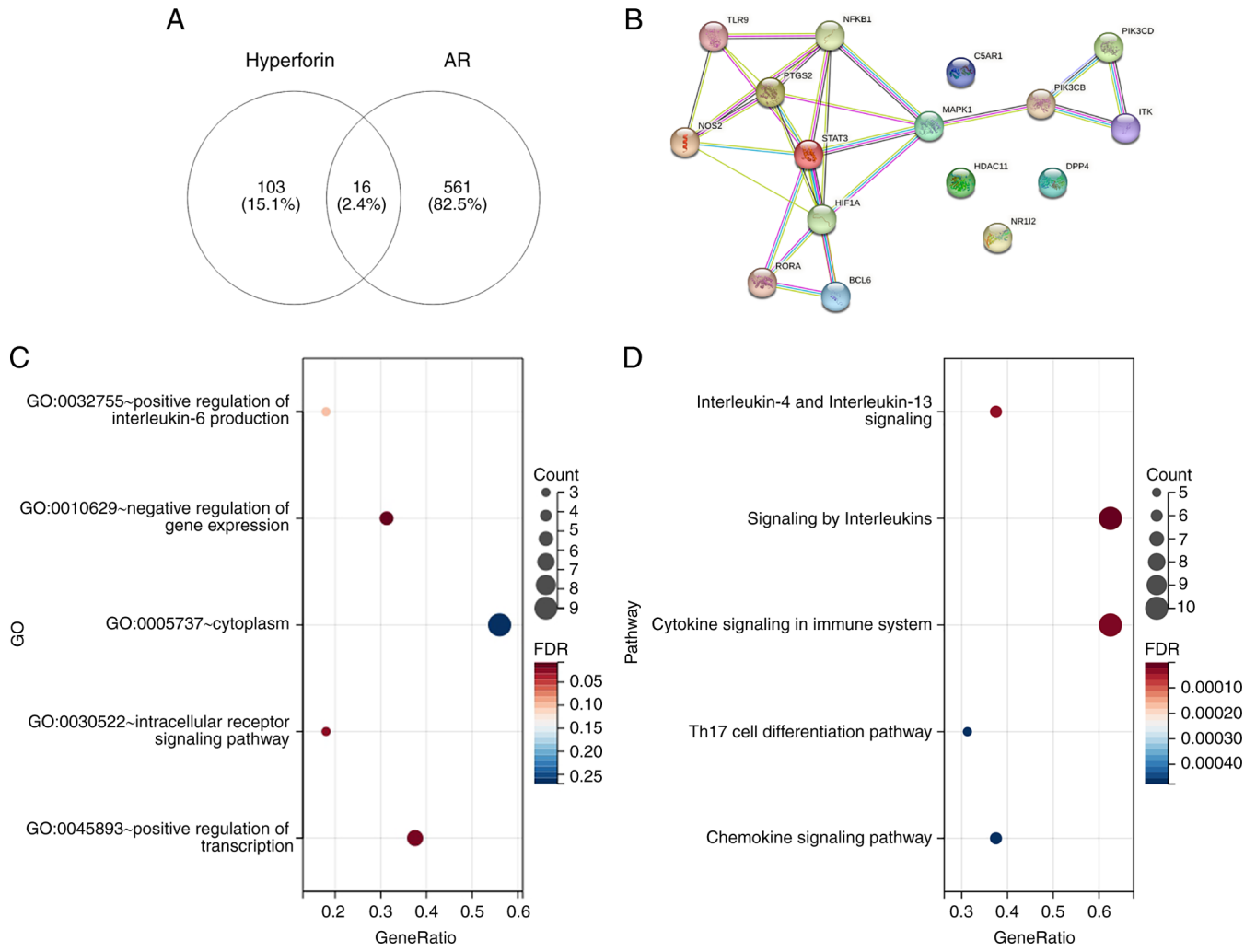

Figure 1. Analysis of intersection genes between hyperforin and AR. (A) Intersection genes of hyperforin and AR were obtained using Venn diagrams. (B) Network of 16 intersection genes of hyperforin and AR was presented using the String database. Analysis of 16 intersection genes by the (C) GO and (D) Pathway databases. AR, allergic rhinitis; GO, Gene Ontology.

mechanism by which hyperforin influences nasal epithelial cell viability, inflammation and barrier damage.

Materials and methods

Bioinformatics analysis. SWISS TargetPrediction (http://www.swisstargetprediction.ch/) was used to identify the potential target genes of hyperforin, while DisGeNET (https://www.disgenet.org/) was used to identify AR target genes. Intersection genes were obtained through Venn diagrams (https://bioinfogp.cnb.csic.es/), and the network was presented using the STRING database (https://cn.string-db.org/). The intersection genes were analyzed by Gene Ontology (GO) (http://geneontology.org/) and Pathway (genome.jp/kegg/) databases. AutoDockTools 1.5.6 software (https://autodock.scripps.edu/) was applied to process proteins, while Discovery Studio 4.5 software (BIOVIA) was used to visualize the results from the molecular docking analyses to obtain 2- and 3D images.

Cell culture and treatment. The human nasal epithelial cell line JME/CF15 was obtained from the Cell Bank of Type Culture Collection of the Chinese Academy of Sciences and cultured in DMEM/F12 (Gibco; Thermo Fisher Scientific, Inc.) supplemented with 10% fetal bovine serum (HyClone; Cytiva) and 1% penicillin/streptomycin in a humidified atmosphere with 5% CO_2 at 37˚C. JME/CF15 cells were treated with 10 ng/ml IL-13 (cat. no. HY-P7033; MedChemExpress) at 37˚C for 30 min (15), with or without treatment with hyperforin at doses of 0.1, 1 and 10 μM for 24 h [the doses of hyperforin were selected referring to previous study (13)].

Cell transfection. Specific small interfering RNA (siRNA) targeting B-cell lymphoma 6 (BCL6) (siRNA-BCL6-1 forward, 5'-GCGUCAUGCUUGUGUUAUAAC-3', and reverse, 5'-UAUAACACAAGCAUGACGCAG-3'; siRNA-BCL6-2 forward, 5'-GGUGGUUGAAGCUGGUUAAAG-3', and reverse: 5'-UUAACCAGCUUCAACCACCAG-3') and the corresponding scrambled negative control (NC) siRNA (siRNA-NC forward, 5'-UUCUCCGAACGUGUCACGU-3' and reverse, 5'-ACGUGACACGUUCGGAGAA-3') were synthesized by Shanghai GenePharma Co., Ltd. A total of 100 nM siRNAs were transfected into JME/CF15 cells using Lipofectamine® 2000 reagent (Invitrogen; Thermo Fisher Scientific, Inc.)

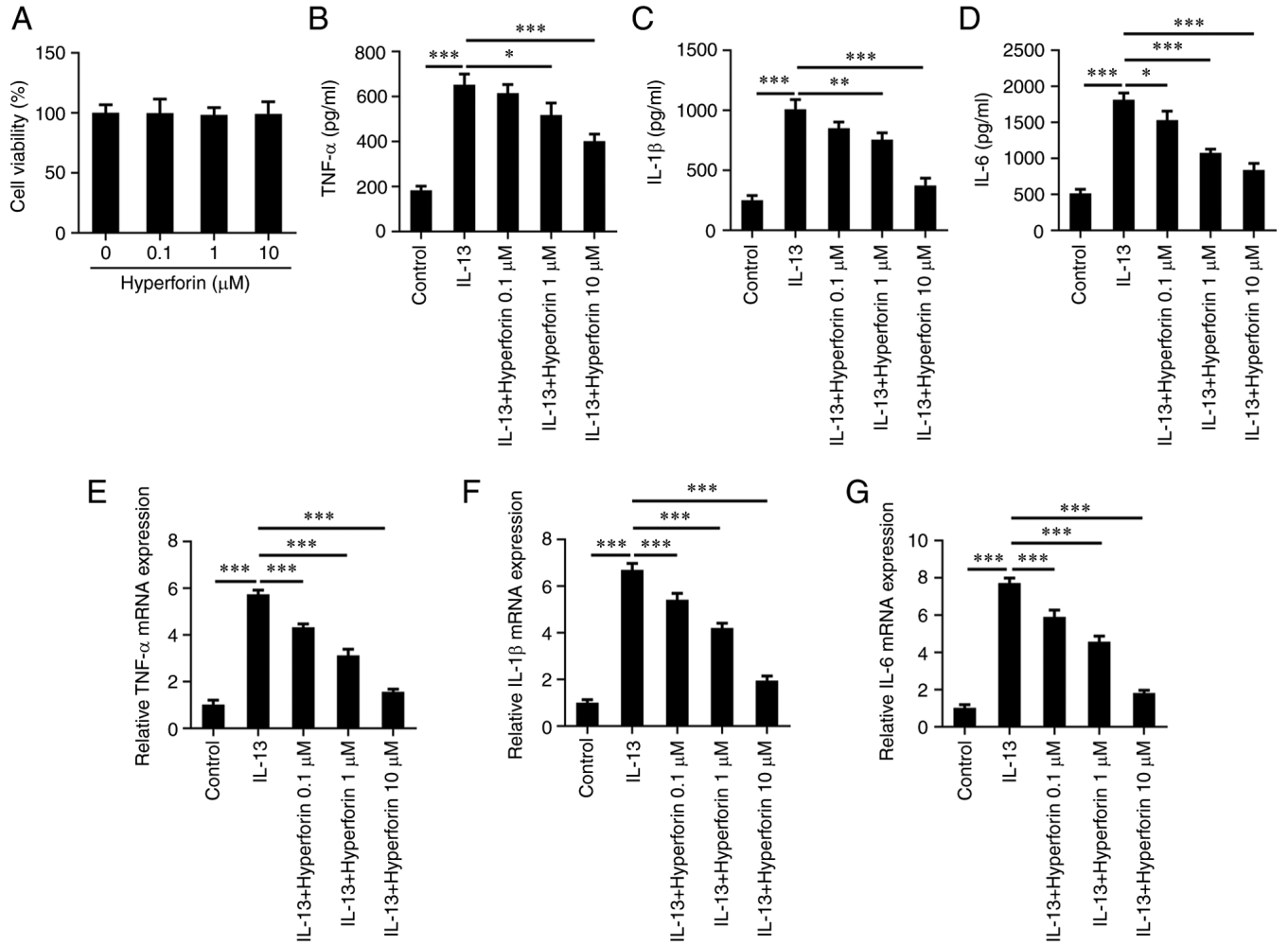

Figure 2. Hyperforin suppresses the release of nasal epithelial inflammatory cytokines induced by IL-13. (A) JME/CF15 cell viability was assessed using Cell Counting Kit-8 assay. The protein levels of (B) TNFα, (C) IL-1β and (D) IL-6 were evaluated using ELISA. The mRNA levels of (E) TNFα, (F) IL-1β and (G) IL-6 were evaluated using reverse transcription-quantitative PCR. *P<0.05, **P<0.01, ***P<0.001.

according to the manufacturer's instructions. After 48 h of transfection, cells were harvested for subsequent experiments.

Cell Counting Kit-8 (CCK-8) assay. JME/CF15 cells were seeded into 96-well plates at a density of $5x10^4$ cells/ml, treated with different doses of hyperforin (0.1, 1 and 10 μM) and cultured at 37˚C for 24 h. Next, 10 μl of WST-8 (Beyotime Institute of Biotechnology) was added to each well and the plates were incubated at 37˚C for 2 h. The absorbance value at 450 nm was measured with a microplate reader (Bio-Rad Laboratories, Inc.).

ELISA. The concentrations of TNFα, IL-1β, IL-6 and CCL11 in JME/CF15 cells were determined by ELISA assay kits related to TNFα (cat. no. F3768), IL-6 (cat. no. F3743) and IL-1β (cat. no. F3739; all from Shanghai Westang Biotechnology Co., Ltd.) according to the manufacturer's protocols. The absorbance was measured at 450 nm with a microplate reader (BioTek Instruments, Inc.).

RNA extraction and reverse transcription-quantitative PCR (RT-qPCR). Total RNA was extracted from JME/CF15 cells by TRIzol® reagent (Invitrogen; Thermo Fisher Scientific, Inc.) in accordance with the manufacturer's protocol. NanoDrop 3000 spectrophotometer (NanoDrop Technologies; Thermo Fisher Scientific, Inc.) was used according to the manufacturer's protocol to confirm the quality of total RNA. cDNA Synthesis Kit (Takara Bio, Inc.) was used to reverse transcribe 2 μg RNA into cDNA at 37˚C for 15 min and 85˚C for 5 sec. Next, amplification of cDNA was performed by real-time qPCR using the SYBR Premix Ex Taq™ II kit (Takara Bio, Inc.). The primer sequences for PCR were as follows: TNF-α, 5'-GACAAGCCTGTAGCCCATGT-3' (forward) and 5'-GGAGGTTGACCTTGGTCTGG-3' (reverse); IL-1β, 5'-AACCTCTTCGAGGCACAAGG-3' (forward) and 5'-AGATTCGTAGCTGGATGCCG-3' (reverse); IL-6, 5'-CCTTCGGTCCAGTTGCCTT-3' (forward) and 5'-ATTTGTGGTTGGGTCAGGGG-3' (reverse); BCL6, 5'-CCCACTCCCATGTGTCTTCA-3' (forward) and 5'-CGGCTCCAAGGTTAGTGTGT-3' (reverse); GAPDH, 5'-GGGAAACTGTGGCGTGAT-3' (forward) and 5'-GAGTGGGTGTCGCTGTTGA-3' (reverse). The thermocycling conditions were as follows: Initial denaturation at 95˚C for 3 min; followed by 40 cycles of denaturation at 95˚C for 30 sec, annealing at 60˚C for 30 sec and extension at 72˚C for 30 sec. The relative mRNA level was normalized with GAPDH using the $2^{-\Delta\Delta Cq}$ method (16).

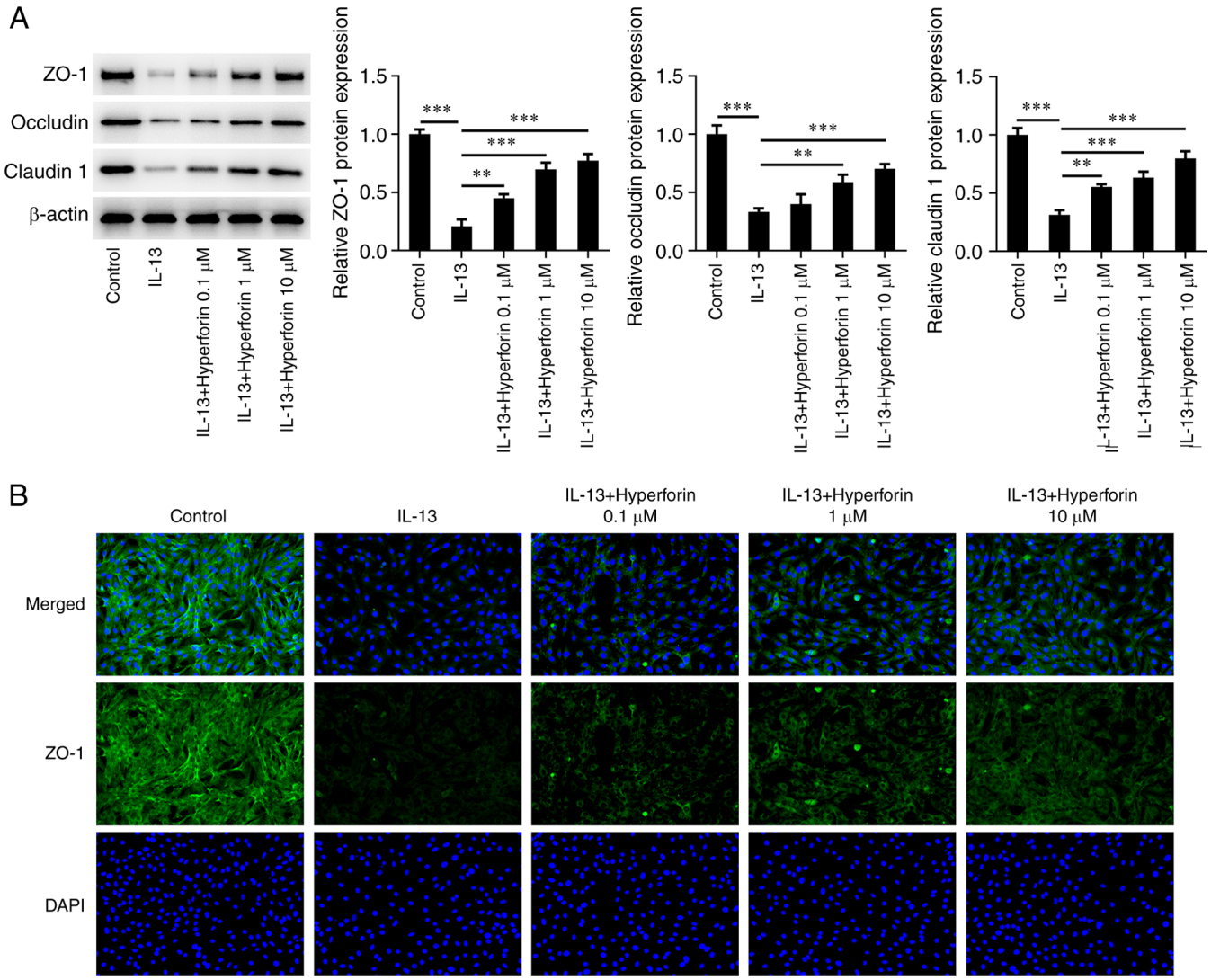

Figure 3. Hyperforin restrains IL-13-induced JME/CF15 cell barrier damage. (A) Protein levels of ZO-1, occludin and claudin 1 in JME/CF15 cells were measured using western blotting. (B) Immunofluorescence staining was used to detect the level of ZO-1 in IL-13-induced cells with or without hyperforin (magnification, x200). **P<0.01, ***P<0.001. ZO-1, zonula occludens-1.

Immunofluorescence staining. Following hyperforin treatment and indicated transfection, IL-13-induced JME/CF15 cells were fixed in 4% polyoxymethylene for 30 min at room temperature and permeabilized with 0.5% Triton-X100 for 7 min at room temperature. After blocking with 2% BSA for 1 h at room temperature, cells were incubated with a primary antibody against zonula occludens-1 (ZO-1; 1:100; cat. no. ab221547; Abcam) at 4˚C overnight. Next, goat anti-rabbit IgG H&L (Alexa Fluor® 488) secondary antibody (1:400; cat. no. ab150077; Abcam) was added and incubated for 1 h at room temperature. The nuclei were stained using a DAPI solution for 5 min at room temperature, and the cells were subsequently visualized under a fluorescence microscope (Eclipse80i; Nikon Corporation).

Western blot analysis. Total proteins were extracted from cells using RIPA buffer (Beyotime Institute of Biotechnology) and quantified using the bicinchoninic acid method (Thermo Fisher Scientific, Inc.). Proteins (20-30 μg per lane) were separated using 10% SDS-PAGE (Bio-Rad Laboratories, Inc.), transferred onto PVDF membranes (MilliporeSigma), and blocked for 1 h in 5% non-fat milk in 0.1% TBS-Tween-20 at room temperature. The membranes were incubated at 4˚C overnight with primary antibodies against ZO-1 (cat. no. ab276131), occludin (cat. no. ab216327), claudin 1 (cat. no. ab211737), BCL6 (cat. no. ab33901), phosphorylated (p)-p38 (cat. no. ab45381) (all from Abcam), p38 (cat. no. AF7668; Beyotime Institute of Biotechnology) and β-actin (1:1,000; cat. no. ab8227; Abcam). Subsequently, the membranes were incubated with HRP-conjugated secondary antibodies (1:5,000; cat. no. ab6721; Abcam) for 1 h at room temperature. Finally, the protein bands were visualized using an ECL detection system (Beyotime Institute of Biotechnology) and quantified using densitometry with Q uantityOne 4.5.0 software (Bio-Rad Laboratories, Inc.).

Statistical analysis. All statistical analyses were conducted using SPSS version 18.0 software (SPSS, Inc.). The results were analyzed by one-way ANOVA followed by Bonferroni's post-hoc test for multiple comparisons. Data are presented

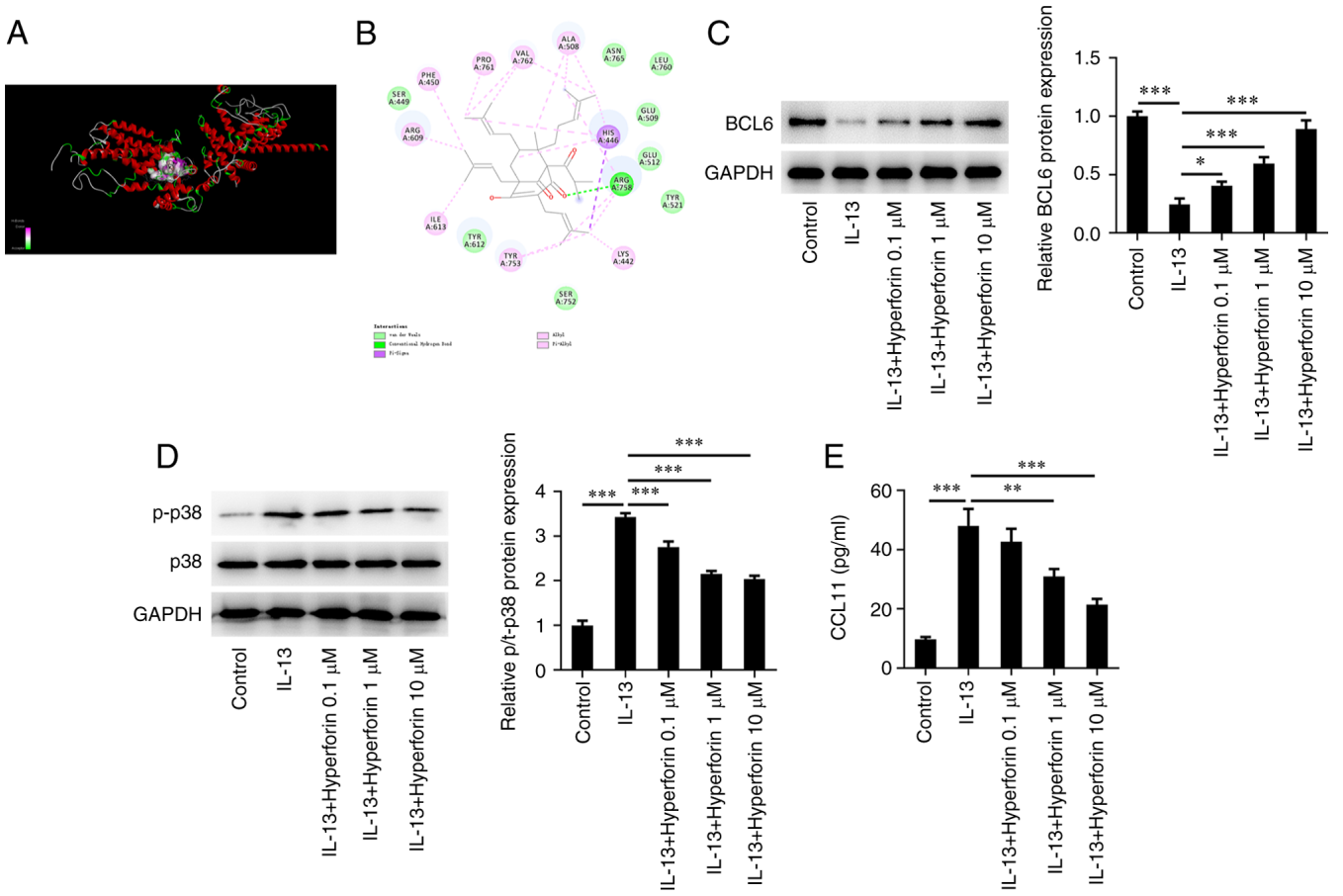

Figure 4. Hyperforin increases BCL6 and inhibits the p38 MAPK/CCL11 pathway in IL-13-induced JME/CF15 cells. Molecular docking (A) 3D and (B) 2D diagram of the binding of hyperforin and BCL6. Western blotting was performed to detect the protein level of (C) BCL6 and (D) p-p38. (E) Protein level of CCL11 was evaluated using ELISA. *P<0.05, **P<0.01, ***P<0.001. BCL6, B-cell lymphoma 6; p-, phosphorylated; CCL11, C-C motif chemokine 11.

as the mean ± standard deviation of three independent experiments. P<0.05 was considered to indicate a statistically significant difference.

Results

Analysis of intersection genes between hyperforin and AR. Using Venn diagrams (https://bioinfogp.cnb.csic.es/), 16 intersection genes of hyperforin and AR were obtained, and the network was presented using the STRING database (https://cn.string-db.org/) (Fig. 1A and B). The intersection genes were then analyzed using the GO and Pathway databases, which demonstrated that the 16 intersection genes were mainly located in the 'cytoplasm', were involved in '(...)regulation of transcription' and were enriched in 'signaling by interleukins'/'cytokine signaling in immune system'/'chemokine signaling pathway'/'IL-4 and IL-13 signaling' (Fig. 1C and D).

Hyperforin suppresses the release of nasal epithelial inflammatory cytokines induced by IL-13. To investigate the effects of hyperforin in AR, the effects of hyperforin on the viability of JME/CF15 cells were first detected. As presented in Fig. 2A, 0.1-100 μM hyperforin had no obvious effects on JME/CF15 cell viability. In addition, ELISA revealed that the protein levels of TNFα, IL-1β and IL-6 in cells treated with IL-13 were significantly increased compared with those of control cells, but treatment with hyperforin reduced the protein levels of TNFα, IL-1β and IL-6 induced by IL-13 in a dose-dependent manner (Fig. 2B-D). Moreover, RT-qPCR also revealed that IL-13 induced the production of TNFα, IL-1β and IL-6, which was reversed by hyperforin treatment (Fig. 2E-G).

Hyperforin restrains IL-13-induced JME/CF15 cell barrier damage. The present study next explored the effects of hyperforin on IL-13-treated JME/CF15 cells and the cell barrier. As presented in Fig. 3A, western blotting revealed that IL-13 significantly reduced the levels of ZO-1, occludin and claudin 1 in JME/CF15 cells compared with the control, while addition of hyperforin increased the IL-13-reduced levels of these three proteins in a dose-dependent manner. In addition, immunofluorescence staining revealed that the number of positive cells in the IL-13 group was decreased, but increased after hyperforin treatment (Fig. 3B).

Hyperforin increases BCL6 and inhibits the p38MAPK/C-C motif chemokine 11 (CCL11) pathway in IL-13-induced JME/CF15 cells. AutoDock software was used to dock hyperforin with the BCL6 protein at the molecular level, and the result revealed that the binding free energy of this active ingredient and BCL6 was -5.8 kcal/mol (Fig. 4A). The molecular docking diagram is presented in Fig. 4B. The expression levels

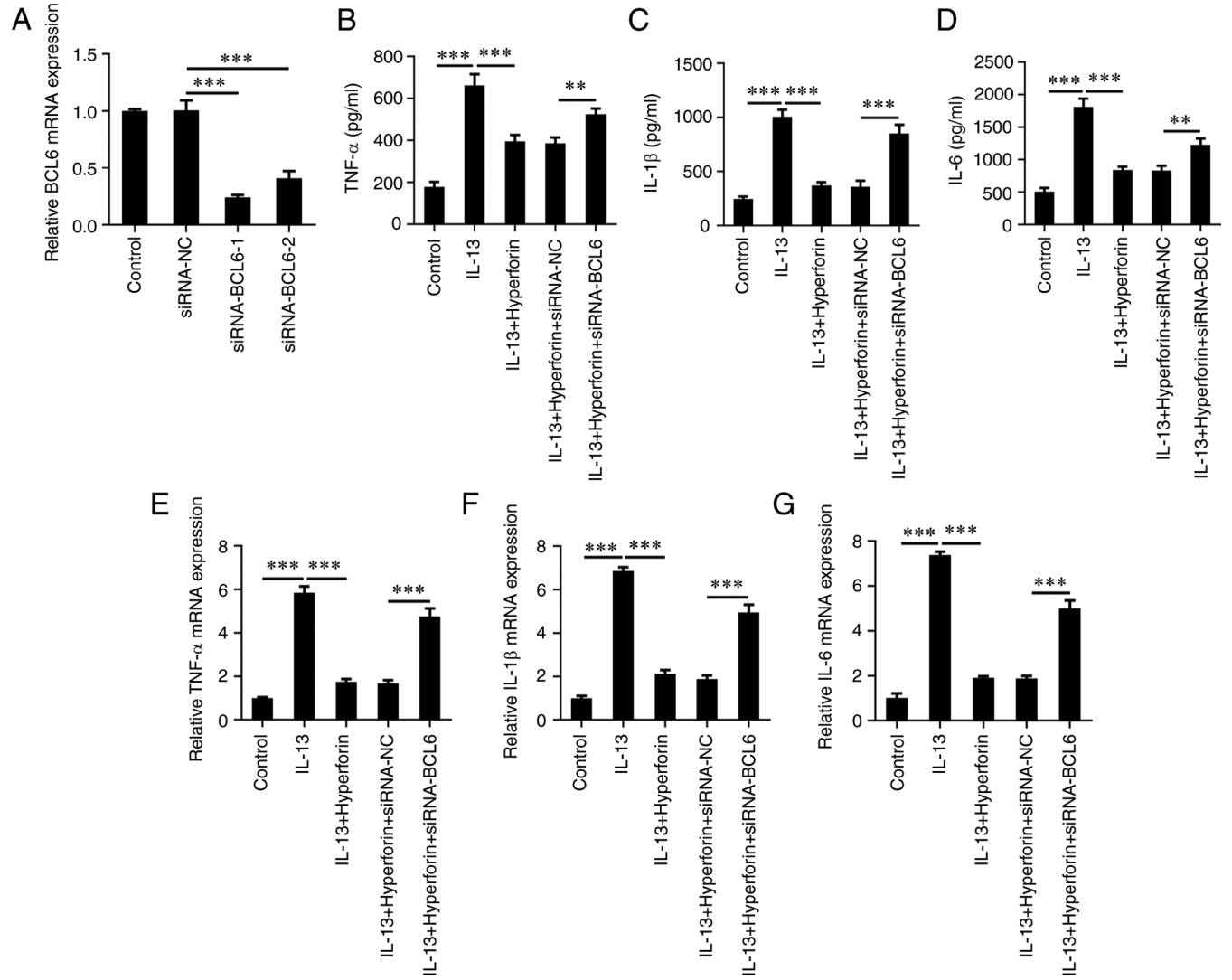

Figure 5. Hyperforin inhibits IL-13-induced nasal epithelial inflammation by activating BCL6. (A) mRNA level of BCL6 was evaluated by RT-qPCR. The protein levels of (B) TNFα, (C) IL-1β and (D) IL-6 were evaluated by ELISA. The mRNA levels of (E) TNFα, (F) IL-1β and (G) IL-6 were evaluated using RT-qPCR. **P<0.01, ***P<0.001. RT-qPCR, reverse transcription-quantitative PCR; BCL6, B-cell lymphoma 6; NC, negative control; siRNA, small interfering RNA.

of molecules associated with the BCL6/p38MAPK/CCL11 pathway were then detected. Western blotting revealed that treatment with IL-13 significantly reduced the protein level of BCL6, which was significantly reversed by treatment with hyperforin in a dose-dependent manner (Fig. 4C). Moreover, IL-13 significantly elevated the levels of p-p38 and CCL11, whereas hyperforin suppressed the expression levels of p-p38 and CCL11 in IL-13-induced cells (Fig. 4D and E).

Hyperforin inhibits IL-13-induced nasal epithelial inflammation and cell barrier damage by activating BCL6. To explore the biological roles of BCL6 in hyperforin-treated AR, siRNA-BCL6-1/2 was transfected to silence BCL6 in JME/CF15 cells. The results demonstrated that siRNA-BCL6-1 had the greater transfection efficiency; thus, siRNA-BCL6-1 (named as siRNA-BCL6) was selected for subsequent assays (Fig. 5A). The results of ELISA demonstrated that co-treatment of hyperforin and BCL6-silencing significantly increased the levels of TNFα, IL-1β and IL-6 in JME/CF15 cells compared with the hyperforin-treated cells alone (Fig. 5B-D). In addition, RT-qPCR also demonstrated the results that BCL6-silencing enhanced the levels of these inflammatory factors compared with the hyperforin-treated cells (Fig. 5E-G). Additionally, siRNA-BCL6 significantly inhibited the production of ZO-1, occludin and claudin 1 in IL-13-induced cells treated with hyperforin (Fig. 6A). Immunofluorescence assay demonstrated the number of positive cells after silencing of BCL6 was notably decreased compared with that in hyperforin-treated cells (Fig. 6B).

Discussion

AR is a growing public health, medical and economic problem worldwide (17). The risk factors for AR include environmental exposure, climate change and lifestyle (18). Although the pathological mechanisms and treatment of AR have been widely researched, numerous aspects of AR remain unclear. At present, management of AR includes patient education, pharmacotherapy, allergen-specific immunotherapy and biologics (19).

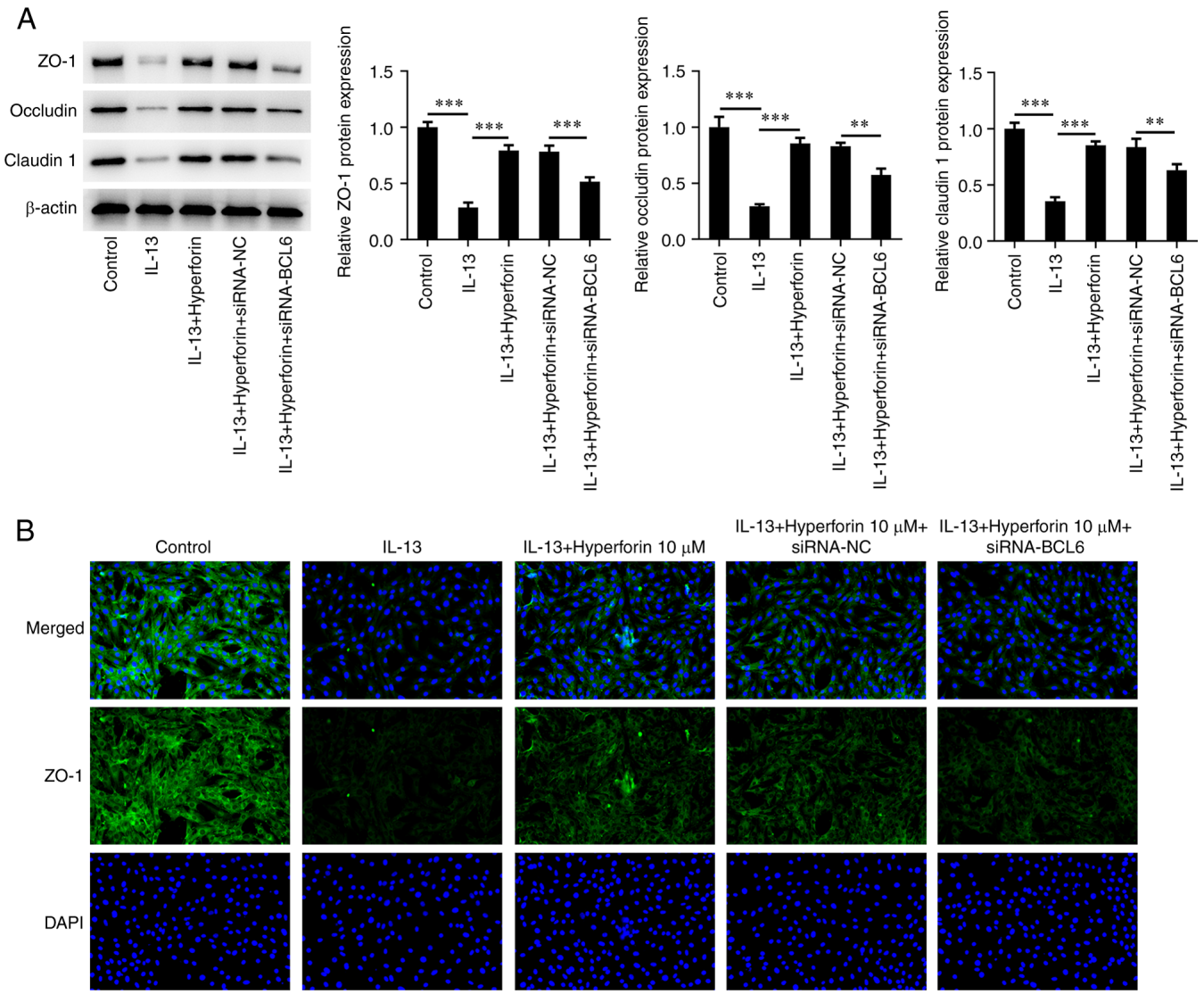

Figure 6. Hyperforin suppresses IL-13-induced nasal epithelial cell barrier damage by activating BCL6. (A) Protein levels of ZO-1, occludin and claudin 1 in JME/CF15 cells were measured by western blotting. (B) Immunofluorescence staining was used to detect the level of ZO-1 in IL-13-induced cells with hyperforin in the presence and absence of siRNA-BCL6. **P<0.01, ***P<0.001. BCL6, B-cell lymphoma 6; ZO-1, zonula occludens-1; NC, negative control; siRNA, small interfering RNA.

Despite the variety of medications for AR, such as glucocorticosteroids, decongestants, histamine receptor and leukotriene blockers and immunotherapy, multiple patients still experience treatment failures or unsatisfactory results (20). Emerging evidence had demonstrated that allergic diseases, including AR, are often caused by numerous inflammatory mediators such as histamine, chemokines and cytokines from immune cells (21,22). IL-13 has been demonstrated to promote mucus production and the secretion of inflammatory cytokines in AR (23). The present study aimed to determine the therapeutic potential of hyperforin in AR cell inflammation and barrier function, and the molecular mechanisms underlying its function. AR is mostly affected by genetics and immunity; however, it is currently hypothesized that rhinitis can be treated with medication or surgery to relieve symptoms (24). The present study revealed the protective effects of hyperforin on the inflammatory response and barrier injury in IL-13-treated nasal mucosal epithelial cells, which revealed that hypericin may be a novel alternative drug used to treat AR.

Hyperforin is a pharmacologically active component of the medicinal plant *Hypericum perforatum*, and has been reported to exhibit anti-inflammatory activity and resistance to barrier damage (25-27). Novelli *et al* (23) reported that hyperforin protects pancreatic β cells *in vitro* against the deleterious effects of immune and inflammatory cytokines by inhibiting multiple phosphorylation steps of cytokine signaling. In addition, hyperforin reduces inflammatory cell infiltration in the spinal cord, and promotes the differentiation of regulatory T cells and Th2 cells by adjusting their master transcription factors to reduce the severity of autoimmune encephalomyelitis (9). Moreover, hyperforin has been reported to promote wound healing and to function as a topical medication for atopic dermatitis (28,29). Takada *et al* (26) also revealed that hyperforin/2-hydroxypropyl-β-cyclodextrin recovers impaired Ca^{2+} responses in the atopic epidermis, which may facilitate wound closure. The current study revealed that hyperforin (0.1-100 μM) had no obvious effects on human nasal epithelial JME/CF15 cell

viability, and hyperforin significantly reduced the release of inflammatory cytokines induced by IL-13 and withstood the barrier damage.

According to bioinformatics analysis, 16 genes were revealed to be associated with hyperforin and AR. BCL6 was the one of these genes, and enrichment analysis demonstrated that BCL6 was enriched in 'interleukin-4 and interleukin-13 signaling', 'signaling by interleukins' and 'cytokine signaling in immune system'. BCL6 is a sequence-specific transcriptional regulator that inhibits the transcription of target genes by binding to a specific DNA sequence in the promoter region (30). It has been reported that BCL6 is expressed in human nasal mucosal epithelial cells, and the expression of BCL6 is decreased in the nasal mucosa of patients with AR (31). Chen *et al* (29) reported that BCL6 suppresses the inflammatory response and attenuates renal inflammation by negatively regulating the transcription of NLRP3 in human renal tubular epithelial cells, indicating the importance of BCL6 in the regulation of human inflammation diseases. The present study used AutoDock software to dock hyperforin with BCL6 protein successfully. It was revealed that treatment with hyperforin increased the expression of BCL6, while silencing of BCL6 reversed the inhibitory effects of hyperforin on IL-13-induced nasal epithelial cell inflammation and barrier injury.

BCL6 can negatively regulate the expression of p38MAPK signaling molecules (32). In addition, p38 has been reported to be involved in AR injury and to activate the downstream expression of CCL11 (33-35). Therefore, it was hypothesized whether hyperforin could inhibit p38MAPK/CCL11 signaling by activating BCL6 to participate in IL-13-induced AR injury. The present results demonstrated that IL-13 enhanced the expression of p-p38 and CCL11 in JME/CF15 cells, and hyperforin inhibited the production of p-p38 and CCL11 induced by IL-13, which was consistent with the aforementioned hypothesis. However, there are several limitations in the present study. The association between BCL6 and AR was demonstrated and rescue experiments were also performed. However, no animal experiments were performed in the current study, and, therefore, relevant animal experiments will be performed in the future. Moreover, the present study did not explore the separate effects of hyperforin on AR inflammation and barrier injury, and this will be explored in the future.

In conclusion, the present results demonstrated that hyperforin reduced inflammatory response and barrier injury in IL-13-treated nasal mucosal epithelial cells by downregulating p38 MAPK/CCL11 signaling by targeting BCL6, which may provide a novel insight into prospective novel strategies for AR therapy.

Acknowledgements

Not applicable.

Funding

The present study was supported by the Wuhan Medical Research Project (grant nos. WZ21Q05 and WZ20M01).

Availability of data and materials

All data generated and/or analyzed during this study are included in this published article.

Authors' contributions

CX and WS designed the study, performed the experiments and drafted and revised the manuscript. CX analyzed the data and searched the literature. CX and WS confirm the authenticity of all the raw data. All authors have read and approved the final manuscript.

Ethics approval and consent to participate

Not applicable.

Patient consent for publication

Not applicable.

Competing interests

The authors declare that they have no competing interests.

References

1. Schuler Iv CF and Montejo JM: Allergic rhinitis in children and adolescents. Pediatr Clin North Am 66: 981-993, 2019.
2. Schuler Iv CF and Montejo JM: Allergic rhinitis in children and adolescents. Immunol Allergy Clin North Am 41: 613-625, 2021.
3. Hoyte FCL and Nelson HS: Recent advances in allergic rhinitis. F1000Res 7: 1333, 2018.
4. Siddiqui ZA, Walker A, Pirwani MM, Tahiri M and Syed I: Allergic rhinitis: Diagnosis and management. Br J Hosp Med (Lond) 83: 1-9, 2022.
5. Incorvaia C, Cavaliere C, Frati F and Masieri S: Allergic rhinitis. J Biol Regul Homeost Agents 32 (1 Suppl 1): S61-S66, 2018.
6. Meng Y, Wang C and Zhang L: Advances and novel developments in allergic rhinitis. Allergy 75: 3069-3076, 2020.
7. Ghezzi M, Pozzi E, Abbattista L, Lonoce L, Zuccotti GV and D'Auria E: Barrier impairment and Type 2 inflammation in allergic diseases: The pediatric perspective. Children (Basel) 8: 1165, 2021.
8. Liu S, Yu B, Dai J and Chen R: Targeting the biological activity and biosynthesis of hyperforin: A mini-review. Chin J Nat Med 20: 721-728, 2022.
9. Li XX, Yan Y, Zhang J, Ding K, Xia CY, Pan XG, Shi YJ, Xu JK, He J and Zhang WK: Hyperforin: A natural lead compound with multiple pharmacological activities. Phytochemistry 206: 113526, 2023.
10. Wu S, Malaco Morotti AL, Wang S, Wang Y, Xu X, Chen J, Wang G and Tatsis EC: Convergent gene clusters underpin hyperforin biosynthesis in St John's wort. New Phytol 235: 646-661, 2022.
11. Novelli M, Masiello P, Beffy P and Menegazzi M: Protective role of St. John's wort and its components hyperforin and hypericin against diabetes through inhibition of inflammatory signaling: Evidence from in vitro and in vivo studies. Int J Mol Sci 21: 8108, 2020.
12. Nawrot J, Gornowicz-Porowska J, Budzianowski J, Nowak G, Schroeder G and Kurczewska J: Medicinal herbs in the relief of neurological, cardiovascular, and respiratory symptoms after COVID-19 infection a literature review. Cells 11: 1897, 2022.
13. Zhang S, Zhang J, Yu J, Chen X, Zhang F, Wei W, Zhang L, Chen W, Lin N and Wu Y: Hyperforin ameliorates imiquimod-induced psoriasis-like murine skin inflammation by modulating IL-17A-producing γδ T cells. Front Immunol 12: 635076, 2021.
14. Lemmen J, Tozakidis IE and Galla HJ: Pregnane X receptor upregulates ABC-transporter Abcg2 and Abcb1 at the blood-brain barrier. Brain Res 1491: 1-13, 2013.

15. Wang B, Gao Y, Zheng G, Ren X, Sun B, Zhu K, Luo H, Wang Z and Xu M: Platycodin D inhibits interleukin-13-induced the expression of inflammatory cytokines and mucus in nasal epithelial cells. Biomed Pharmacother 84: 1108-1112, 2016.
16. Livak KJ and Schmittgen TD: Analysis of relative gene expression data using real-time quantitative PCR and the 2(-Delta Delta C(T)) method. Methods 25: 402-408, 2001.
17. Kakli HA and Riley TD: Allergic rhinitis. Prim Care 43: 465-475, 2016.
18. Campo P, Eguiluz-Gracia I, Bogas G, Salas M, Plaza Serón C, Pérez N, Mayorga C, Torres MJ, Shamji MH and Rondon C: Local allergic rhinitis: Implications for management. Clin Exp Allergy 49: 6-16, 2019.
19. Zhang Y, Lan F and Zhang L: Advances and highlights in allergic rhinitis. Allergy 76: 3383-3389, 2021.
20. Beken B, Eguiluz-Gracia I, Yazıcıoğlu M and Campo P: Local allergic rhinitis: A pediatric perspective. Turk J Pediatr 62: 701-710, 2020.
21. Wang L, Lv Q, Song X, Jiang K and Zhang J: ADRB2 suppresses IL-13-induced allergic rhinitis inflammatory cytokine regulated by miR-15a-5p. Hum Cell 32: 306-315, 2019.
22. Teng Y, Zhang R, Liu C, Zhou L, Wang H, Zhuang W, Huang Y and Hong Z: miR-143 inhibits interleukin-13-induced inflammatory cytokine and mucus production in nasal epithelial cells from allergic rhinitis patients by targeting IL13Rα1. Biochem Biophys Res Commun 457: 58-64, 2015.
23. Novelli M, Menegazzi M, Beffy P, Porozov S, Gregorelli A, Giacopelli D, De Tata V and Masiello P: St. John's wort extract and hyperforin inhibit multiple phosphorylation steps of cytokine signaling and prevent inflammatory and apoptotic gene induction in pancreatic β cells. Int J Biochem Cell Biol 81: 92-104, 2016.
24. Pavón-Romero GF, Parra-Vargas MI, Ramírez-Jiménez F, Melgoza-Ruiz E, Serrano-Pérez NH and Teran LM: Allergen immunotherapy: Current and future trends. Cells 11: 212, 2022.
25. Meinke MC, Schanzer S, Haag SF, Casetti F, Müller ML, Wölfle U, Kleemann A, Lademann J and Schempp CM: In vivo photoprotective and anti-inflammatory effect of hyperforin is associated with high antioxidant activity in vitro and ex vivo. Eur J Pharm Biopharm 81: 346-350, 2012.
26. Takada H, Yonekawa J, Matsumoto M, Furuya K and Sokabe M: Hyperforin/HP-β-cyclodextrin enhances mechanosensitive Ca^{2+} signaling in HaCaT keratinocytes and in atopic skin ex vivo which accelerates wound healing. Biomed Res Int 2017: 8701801, 2017.
27. Brondz I: Super antibiotics, part II. Hyperforin, mass spectroscopy (MS) and gas chromatography-mass spectrometry (GC-MS), evidence of permeability of the blood-testis barrier (BTB) and the blood-brain barrier (BBB) to hyperforin. Int J Anal Mass Spectrom Chromatogr 4: 66-73, 2016.
28. Marrelli M, Statti G, Conforti F and Menichini F: New potential pharmaceutical applications of hypericum species. Mini Rev Med Chem 16: 710-720, 2016.
29. Chen D, Xiong XQ, Zang YH, Tong Y, Zhou B, Chen Q, Li YH, Gao XY, Kang YM and Zhu GQ: BCL6 attenuates renal inflammation via negative regulation of NLRP3 transcription. Cell Death Dis 8: e3156, 2017.
30. Béguelin W, Teater M, Gearhart MD, Calvo Fernández MT, Goldstein RL, Cárdenas MG, Hatzi K, Rosen M, Shen H, Corcoran CM, *et al*: EZH2 and BCL6 cooperate to assemble CBX8-BCOR complex to repress bivalent promoters, mediate germinal center formation and lymphomagenesis. Cancer Cell 30: 197-213, 2016.
31. Peng Y, Li XQ and Qiu QH: Detection of differentially expressed gene of allergic rhinitis based on RT^2 profiler PCR array. Lin Chuang Er Bi Yan Hou Tou Jing Wai Ke Za Zhi 31: 869-872, 2017 (In Chinese).
32. Gu Y, Luo M, Li Y, Su Z, Wang Y, Chen X, Zhang S, Sun W and Kong X: Bcl6 knockdown aggravates hypoxia injury in cardiomyocytes via the P38 pathway. Cell Biol Int 43: 108-116, 2019.
33. Long S and Zhang H: MIR-181A-5P attenuates ovalbumin-induced allergic inflammation in nasal epithelial cells by targeting IL-33/P38 MAPK pathway. Clin Invest Med 44: E31-E38, 2021.
34. Roh KB, Jung E, Park D and Lee J: Fumaric acid attenuates the eotaxin-1 expression in TNF-α-stimulated fibroblasts by suppressing p38 MAPK-dependent NF-κB signaling. Food Chem Toxicol 58: 423-431, 2013.
35. Park JY, Choi JH, Lee SN, Cho HJ, Ahn JS, Kim YB, Park DY, Park SC, Kim SI, Kang MJ, *et al*: Protein arginine methyltransferase 1 contributes to the development of allergic rhinitis by promoting the production of epithelial-derived cytokines. J Allergy Clin Immunol 147: 1720-1731, 2021.